Interdisciplinary Research in Medical Sciences Specialty
ISSN: 3062-4401
2026, Volume 6, Issue 1, Page No: 41-57

Available online at: www.galaxypub.co/page/journals

Galaxy Publication

APOA2-Driven Lipid Metabolic Remodeling Underlies the Therapeutic Effect of Platelet-Derived Apoptotic Vesicles in NAFLD

Krzysztof Wiśniewski[1]*, Małgorzata Nowak[1], Tomasz Adamczyk[2]

[1]Department of Hepatology and Lipid Metabolism, Faculty of Medicine, Warsaw University of Life Sciences, Warsaw, Poland.
[2]Department of Platelet Biology and NAFLD Research, Faculty of Medicine, Jagiellonian University, Krakow, Poland.

***E-mail** ✉ krzysztof.wisniewski@sggw.edu.pl

Received: 12 January 2026; **Revised:** 24 March 2026; **Accepted:** 04 April 2026

ABSTRACT

Nonalcoholic fatty liver disease (NAFLD) represents a spectrum of hepatic disorders that begins with simple steatosis and can advance to nonalcoholic steatohepatitis, potentially progressing further to fibrosis, cirrhosis, and hepatocellular carcinoma. At present, no pharmacological agent has received approval for the treatment of NAFLD-related hepatic steatosis. This situation highlights the urgent requirement for more effective interventions capable of modulating lipid metabolism and preventing the advancement from steatosis to more severe chronic liver conditions. Previous investigations have shown that apoptotic vesicles (apoVs) generated during programmed cell death hold considerable promise in maintaining liver homeostasis. Nevertheless, their capacity to alleviate NAFLD remains unexplored. In the current study, apoVs derived from platelets (PLT-apoVs) and from mesenchymal stem cells (MSC-apoVs) were administered in models of NAFLD. PLT-apoVs demonstrated more pronounced efficacy in reducing high-fat diet-induced hepatic lipid accumulation than MSC-apoVs. Proteomic profiling identified and confirmed apolipoprotein A-II (APOA2) as a critical mediator of apoV-regulated adipogenesis in MSCs, positioning it as a promising target for optimizing apoV-based therapies in lipid metabolism disorders. The elevated APOA2 content in PLT-apoVs accounted for their superior therapeutic performance relative to MSC-apoVs. These findings establish a foundation for the development of apoV-based strategies in the management of NAFLD.

Keywords: Apolipoprotein A-II, Apoptotic vesicles, Nonalcoholic fatty liver disease, Platelets

How to Cite This Article: Wiśniewski K, Nowak M, Adamczyk T. APOA2-Driven Lipid Metabolic Remodeling Underlies the Therapeutic Effect of Platelet-Derived Apoptotic Vesicles in NAFLD. Interdiscip Res Med Sci Spec. 2026;6(1):41-57. https://doi.org/10.51847/idqAfolV3P

Introduction

Nonalcoholic fatty liver disease (NAFLD) constitutes a major worldwide public health challenge, affecting approximately one-quarter of the global population [1, 2]. The condition spans a continuum that includes nonalcoholic steatohepatitis (NASH), nonalcoholic fatty liver (NAFL), and associated complications such as hepatic fibrosis and cirrhosis [3, 4]. Key drivers of inflammation, steatosis, and hepatocyte injury involve impaired fatty acid β-oxidation and increased de novo lipogenesis in the liver [5]. Therapeutic development for NAFLD has explored multiple categories of agents, including metabolic regulators such as GLP-1 receptor agonists and FGF21 analogs, which show potential for decreasing hepatic fat content or fibrosis [6, 7]; anti-inflammatory compounds targeting inflammatory cascades [8, 9]; and interventions modulating the gut microbiota [10, 11]. Growing interest has also focused on natural products, supported by preclinical data and their generally favorable safety characteristics [12]. However, challenges including drug-drug interactions, variable metabolic handling, and potential toxicity limit their clinical application [12-14]. Currently, no approved pharmacological treatments exist specifically for preventing or reversing hepatic steatosis in NAFLD [15]. Consequently, there remains a

critical demand for novel therapeutic modalities that effectively control lipid homeostasis and impede progression to advanced liver disease.

Mesenchymal stem cells (MSCs) are readily obtainable from various tissues and exhibit robust self-renewal and multilineage differentiation capabilities [16]. Multiple lines of evidence indicate that MSCs contribute to liver homeostasis and may exert beneficial effects in NAFLD [17, 18]. Nevertheless, clinical translation of MSC therapy is hindered by high costs and logistical complexities associated with stringent quality control during production, processing, and cryopreservation to ensure cell viability and functionality after transplantation [19, 20]. Additionally, transplanted MSCs undergo substantial apoptosis in vivo, raising concerns about the long-term safety of apoptotic cell administration [21].

Apoptotic vesicles (apoVs) are nanoscale, membrane-bound particles released during apoptosis, characterized by diverse biogenesis pathways, sizes, and molecular payloads [22, 23]. These vesicles carry a rich assortment of bioactive molecules—including proteins, lipids, DNAs, RNAs, and metabolites—that facilitate multiple forms of intercellular communication [24, 25]. ApoVs address several limitations of live MSC therapy by reducing immunogenicity and improving stability [26], enhancing delivery precision and safety [27], and enabling efficient loading of therapeutic agents [28]. Earlier work from our group demonstrated that systemic administration of apoVs effectively supports liver homeostasis [19, 29]. However, their therapeutic potential in NAFLD has not yet been determined.

For clinical-scale production, apoVs can be efficiently generated from highly proliferative cell types such as MSCs [30]. Prior studies have shown that MSC-apoVs restore liver macrophage homeostasis through efferocytosis [31] and support hepatic regeneration [27]. Despite these advantages, prolonged cell culture can compromise cellular and vesicular function, and residual nuclear components raise immunological concerns [32, 33]. Therefore, apoV subpopulations that bypass extensive cell expansion and lack nuclear material may offer superior translational prospects. Recent attention has turned to platelet-derived extracellular vesicles [25], although traditional isolation methods remain technically demanding and yield insufficient quantities for clinical use. We recently established that platelets can produce abundant apoVs (PLT-apoVs) following induction of apoptosis [32]. These PLT-apoVs were fully characterized, their specific markers identified, and their enhanced capacity for bone regeneration via GOLPH2-AKT pathway activation confirmed [32]. Several practical advantages favor the use of platelets over MSCs as a source for apoV production: (1) large supplies of clinical-grade allogeneic platelets are routinely available from blood banks; (2) the anucleate nature and avoidance of cell expansion reduce safety risks; and (3) elimination of culture-derived contaminants lowers the potential for impurities [32]. To establish the utility of apoVs in lipid metabolism regulation, it is essential to compare outcomes between PLT-apoV and MSC-apoV treatments. Accordingly, the present study evaluated their relative therapeutic efficacy in NAFLD models and confirmed the superior performance of PLT-apoVs in restoring lipid balance. Crucially, apolipoprotein A-II (APOA2) was identified as a pivotal mediator in apoV-directed lipid metabolism, enabling targeted engineering to generate highly effective therapeutic vesicles.

Materials and Methods

Cell culture and adipogenic induction

Primary human mesenchymal stem cells (MSCs) were obtained from ScienCell (USA). Experiments were conducted using MSCs from three independent donors. Cells were maintained in proliferation medium (PM) or subjected to adipogenic induction in adipogenic medium (AM) at 37°C in a humidified atmosphere containing 5% CO_2 and maintained under sterile conditions [24]. PM consisted of Dulbecco's Modified Eagle's Medium (DMEM, Gibco, USA) supplemented with 10% (v/v) fetal bovine serum (FBS, ScienCell, USA) and 1% (v/v) penicillin/streptomycin (Gibco, USA). AM was prepared in DMEM containing 50 nM insulin, 100 nM dexamethasone, 200 μM indomethacin, 500 μM isobutylmethylxanthine, 10% (v/v) FBS, and 1% (v/v) penicillin/streptomycin. Upon reaching 80%–90% confluence, cells were detached using trypsin (Gibco, USA) and subcultured.

Isolation of platelets

The study protocol was reviewed and approved by the Biomedical Ethics Committee of Peking University School and Hospital of Stomatology (approval number: PKUSSIRB-202170183) and conducted in accordance with the Declaration of Helsinki. All donors provided written informed consent after receiving a full explanation of the

procedures. Peripheral blood was collected by venipuncture from healthy volunteers who had abstained from medication for at least 7 days. Platelets (PLTs) were isolated according to the protocol previously described [32].

Extraction and purification of apoptotic vesicles

Mesenchymal stem cells were washed twice with 0.1 μm-filtered phosphate-buffered saline (PBS) and then treated with 250 nM staurosporine (STS, Enzo Life Sciences, USA) in α-MEM. After 12 hours of incubation, the culture supernatant was collected for apoV isolation. Platelets were washed once with 0.1 μm-filtered PBS and resuspended in α-MEM containing 500 nM STS. Following a 4-hour incubation, the medium containing apoptotic platelets was harvested and apoVs were isolated using the established method [30].

Scanning electron microscopy

For scanning electron microscopy (SEM), samples were fixed in 4% paraformaldehyde (PFA) for 30 minutes and mounted onto silicon wafers. The specimens were then dehydrated through a graded ethanol series and subjected to lyophilization for 8 hours. After platinum sputter-coating, morphological examination was performed using a high-resolution field emission SEM (Quanta FEG 450, FEI, USA) [3].

Cryo-electron microscopy

Cryo-electron microscopy sample preparation followed the approach reported in our previous study [34]. Holey-carbon grids were glow-discharged for 60 seconds prior to use. ApoVs were applied to the grids, excess liquid was blotted away with filter paper, and the grids were plunge-frozen using an FEI Vitrobot Mark IV operated at 4°C and 100% humidity. Images were acquired on an FEI Titan Krios transmission electron microscope (TEM) equipped with a Gatan K2 Summit camera (USA) operating at 300 kV, with a GIF Quantum energy filter (Gatan, USA).

Nanoparticle tracking analysis

To evaluate particle size distribution and zeta potential, apoVs were appropriately diluted in 0.1 μm-filtered PBS and analyzed with a ZetaView PMX120 instrument (Particle Metrix, Germany) [32]. Data processing was performed using ZetaView analysis software (Version 8.02.31).

Nano-flow cytometry

For high-resolution nano-flow cytometric analysis, apoVs were diluted in 0.1 μm-filtered PBS and examined using a Flow NanoAnalyzer (NanoFCM Inc.) according to the manufacturer's instructions [22]. Samples were diluted to achieve particle concentrations within the optimal detection range of 4000–14,000 particles. Particle concentration, size distribution, and the percentage of positively stained particles were determined using NanoFCM software (NanoFCM Profession V1.0).

Proteomic analysis

Protein lysates were prepared as previously described [35]. Proteomic profiling was conducted on a Q-Exactive HF mass spectrometer (Thermo Fisher Scientific, San Jose, CA) employing both data-dependent acquisition and data-independent acquisition modes. Proteins with a fold change ≥ 2 and an adjusted p-value < 0.05 were classified as differentially expressed and subjected to functional enrichment analyses, including Kyoto Encyclopedia of Genes and Genomes (KEGG) pathway and Gene Ontology (GO) analyses.

Cell proliferation assay

To establish a safe working concentration, cells were exposed to a range of apoV concentrations. Culture medium was replaced every 2 days. Cell viability and proliferation were monitored using the Cell Counting Kit-8 (CCK-8, Dojindo, Japan). Growth curves were generated from absorbance readings collected over 0–7 days [36].

Oil red O staining and quantification

Mesenchymal stem cells (MSCs) were maintained in culture under three separate conditions: proliferation medium (PM), adipogenic induction medium (AM), and AM further enriched with apoptotic vesicles (apoV group). The medium was changed at intervals of 2–3 days. Once the 14-day culture period was complete, Oil Red O staining along with quantitative measurement was executed following the established protocol [37]. In the

quantitative procedure, the dye from stained cells was extracted by incubation in 100% isopropyl alcohol for 10 min, after which optical density was determined at 500 nm.

RNA extraction and RT-qPCR

Total RNA from the cells was isolated with TRIzol reagent (Invitrogen, USA) [38]. Reverse transcription to generate cDNA was carried out using the PrimeScript RT reagent kit (Takara, Japan). Quantitative PCR analysis was then performed on an ABI Prism 7500 real-time PCR instrument. Gene expression levels were calculated via the 2–ΔΔCT method, normalized against GAPDH as the housekeeping gene, and reported as relative fold changes.

Western blotting

Proteins were extracted from cells lysed in RIPA buffer (Santa Cruz Biotechnology, USA) containing 2% protease inhibitor cocktail [13, 30]. The extracted proteins were resolved on 10% SDS-PAGE gels (Lablead, China), electrotransferred to polyvinylidene fluoride membranes (Millipore, USA), blocked in 5% non-fat milk prepared in TBST (TBS with 0.1% Tween-20), and incubated overnight at 4°C with primary antibodies. After washing, membranes were exposed to peroxidase-linked secondary antibodies for 1 h at room temperature. Bands were detected with ECL substrate (CoWin Biotech, China) and documented using a Fusion FX6 imaging system (Vilber, France).

Magnetic-activated apoptotic vesicle sorting

Isolation of apoptotic vesicles (apoVs) by magnetic sorting followed a previously reported method [22]. ApoVs were sequentially labeled with APOA2 antibodies (1:1000 dilution, Abcam, UK), PE-conjugated secondary antibodies (Proteintech, USA), and anti-PE MicroBeads (Miltenyi Biotec, Germany). Washing with 0.1 μm-filtered PBS was performed after each labeling step. The suspension was loaded onto a magnetic column, and the flow-through fraction representing the APOA2-negative population was collected.

Lentivirus infection

Lentiviral vectors carrying shRNA were employed to achieve APOA2 overexpression in MSCs, consistent with earlier protocols [39]. Cells were transduced with either control vector or sh-APOA2 construct (Sangon Biotech, China) as recommended by the supplier.

APOA2 incorporation

Naïve apoVs derived from platelets or MSCs were suspended in 0.1 μm-filtered PBS at a total protein concentration of 100 ng/mL [40]. An APOA2 protein solution (0.5 mg/mL in PBS) was added to 250 μL of the apoV suspension to obtain a final total protein concentration of 0.1 mg/mL. The resulting mixture underwent sonication on a Qsonica Sonicator Q700 (Fisher Scientific, Hampton, NH, USA) set at 500 V, 2 kHz, and 20% amplitude, using six cycles of 4 s on and 2 s off. Following sonication, the sample was placed on ice for 2 min and then subjected to an additional round of sonication.

Animals

All experimental animals were sourced from Vital River (China) and housed under specific-pathogen-free conditions at the Peking University School of Stomatology. The animal facility operated on a 12-h light/dark cycle with temperature maintained at 23 ± 3°C. Sterilized chow and autoclaved water were provided ad libitum. All animal procedures were approved in advance by the Institutional Animal Care and Use Committee of Peking University Health Science Center (approval number LA2022039).

Intravenous injection of apoptotic vesicles in high-fat diet mice

Male C57BL/6J mice aged 6–8 weeks were assigned to either high-fat diet (HFD) or regular chow (RC) feeding for 16 weeks [41]. Throughout the feeding regimen, HFD-fed mice received once-weekly tail-vein injections of apoVs, while control animals were administered an equal volume of vehicle (0.1 μm-filtered PBS). At the conclusion of the experiment, mice were anesthetized and euthanized. Internal organs and abdominal adipose tissue were collected, fixed in 4% paraformaldehyde, and subsequently processed for decalcification, embedding, sectioning, and histological staining.

Statistical analysis

All results are presented as mean ± standard deviation (SD) based on data from a minimum of three independent experiments and were statistically evaluated using SPSS 20.0 (IBM, USA). Two-group comparisons were analyzed by independent two-tailed Student's t-test or Welch's corrected t-test. For multiple-group comparisons, one-way ANOVA with Tukey's post hoc test or Welch's ANOVA with Dunnett's T3 post hoc test was utilized. Differences were regarded as statistically significant at $p < 0.05$.

Results and Discussion

Fundamental characteristics of PLT-ApoVs and MSC-ApoVs

Platelet morphology and size distribution were assessed via scanning electron microscopy (SEM), which demonstrated diameters ranging from 1.2 to 2.5 μm, consistent with established literature [1]. The platelets displayed the expected spherical morphology typical of resting, non-activated cells [2]. Consequently, the isolated platelet population exhibited excellent uniformity.

Apoptosis was induced in both platelets (PLTs) and mesenchymal stem cells (MSCs) through staurosporine (STS) treatment [32]. In brief, each blood collection of 2 mL yielded approximately 2 × 10^8 PLTs. These platelets subsequently produced an average of 3.85 × 10^11 PLT-derived apoptotic vesicles (PLT-apoVs), equating to roughly 1925 vesicles per individual platelet. Comprehensive characterization of the isolated apoVs was performed using cryo-electron microscopy (Cryo-EM), nanoparticle tracking analysis (NTA), flow cytometry, and western blotting. Cryo-EM images confirmed that both PLT-apoVs and MSC-apoVs presented as intact spherical particles bounded by a continuous membrane **(Figure 1a)**. NTA measurements showed particle sizes spanning 10 to 1000 nm, with median diameters of 151.1 nm for PLT-apoVs and 163.5 nm for MSC-apoVs **(Figure 1b)**. Mean zeta potentials were determined to be −24.64 mV and −25.38 mV for PLT-apoVs and MSC-apoVs, respectively **(Figure 1c)**. Flow cytometric evaluation verified externalization of phosphatidylserine on their surfaces **(Figure 1d)**. Both western blot and flow cytometry data confirmed strong expression of specific apoV markers (ITGA5, RhoA, RPS25, and Lamin B1) along with standard extracellular vesicle markers (TSG101 and CD9) **(Figures 1e–1f)**, corroborating earlier findings [22].

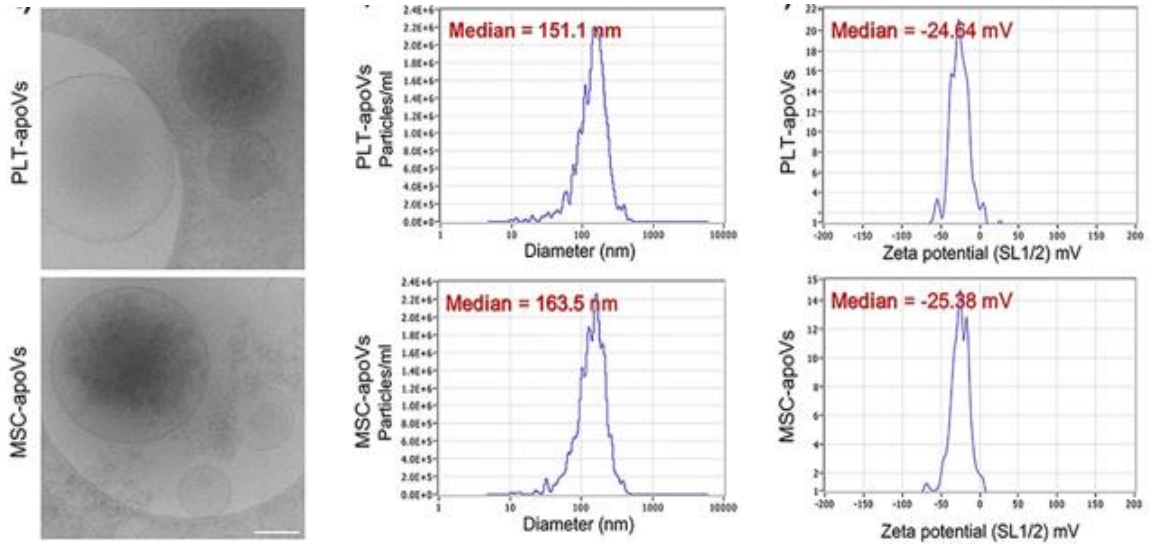

a) b) c)

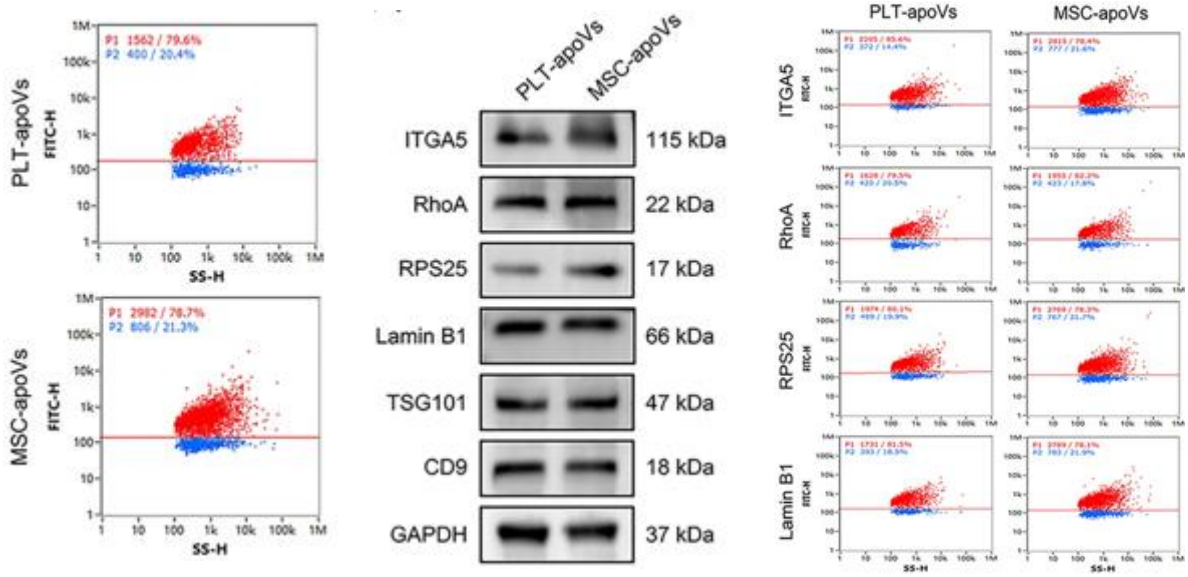

d) e) f)

Figure 1. Morphological and biochemical features of PLT-apoVs and MSC-apoVs. (a) Representative Cryo-EM images illustrating apoV structure. Scale bar: 50 nm. (b) Size distribution profiles of apoVs determined by Zetaview. (c) Zeta potential measurements of apoVs obtained via Zetaview. (d) Assessment of phosphatidylserine surface exposure on apoVs by nano-flow cytometry. (e) Western blot detection of apoV markers (ITGA5, RhoA, RPS25, and Lamin B1) and EV markers (TSG101 and CD9). (f) Quantification of apoV marker positivity rates (ITGA5, RhoA, RPS25, and Lamin B1) using nano-flow cytometry. apoV, apoptotic vesicle.

Proteomic analysis of PLT-ApoVs and MSC-ApoVs

Protein extracts were prepared from both PLT-apoVs and MSC-apoVs, followed by mass spectrometry-based proteomic profiling in accordance with previously validated methodologies [32]. The apoVs originated from platelets of three independent healthy donors and MSCs from three distinct donors. In total, approximately 8200 proteins were confidently identified across the samples. Comparative analysis identified 1574 proteins significantly upregulated and 3029 proteins significantly downregulated in PLT-apoVs relative to MSC-apoVs **(Figures 2a and 2b)**.

Functional pathway enrichment was performed focusing on the proteins elevated in PLT-apoVs. KEGG analysis (level 2) demonstrated prominent enrichment in “immune system” and “endocrine system” pathways within the organismal systems category, “carbohydrate metabolism” within metabolism, “cancers” and “infectious diseases” within human diseases, “folding, sorting and degradation” within genetic information processing, “signal transduction” within environmental information processing, and “transport and catabolism” within cellular processes **(Figure 2c)**. These observations indicate that PLT-apoVs carry a rich repertoire of proteins implicated in cellular regulation, metabolic control, and disease-related processes. Complementary Gene Ontology (GO) enrichment analysis showed that the upregulated proteins were predominantly associated with the “plasma membrane” and “lipoprotein particle” in the cellular component category, exhibited “calcium ion binding” and “lipase activity” as major molecular functions, and participated extensively in “neutrophil degranulation” and “lipid catabolic process” within biological processes **(Figure 2d)**. This detailed side-by-side proteomic comparison between platelet- and MSC-derived apoptotic vesicles offers new perspectives on their potential differential contributions to metabolic regulation, particularly in lipid homeostasis.

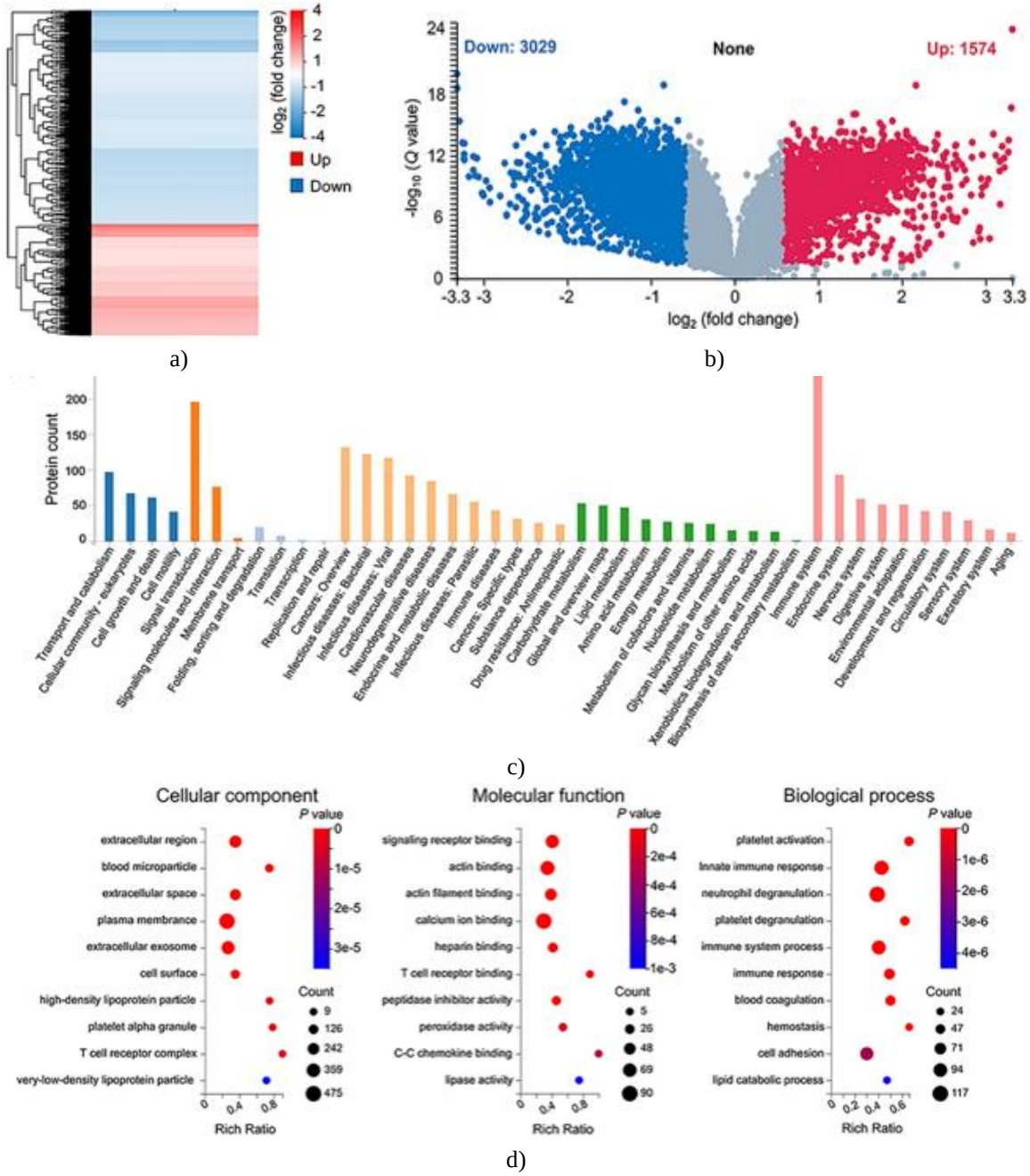

Figure 2. Comparative protein composition of PLT-apoVs and MSC-apoVs.
(a) Heatmap displaying clustering of differentially expressed proteins (DEPs) between PLT-apoVs and MSC-apoVs. DEPs were selected using criteria of fold change ≥ 2 and adjusted p-value < 0.05. The x-axis shows log2 (fold change) values and the y-axis lists proteins. Red indicates enrichment and blue indicates depletion. (b) Volcano plot illustrating upregulated proteins (red) and downregulated proteins (blue) in PLT-apoVs versus MSC-apoVs. (c) KEGG pathway enrichment (level 2) for proteins upregulated in PLT-apoVs. (d) GO enrichment analysis of proteins upregulated in PLT-apoVs. Bar graphs reflect enrichment significance (−log10 (p value)) and the overlaid line indicates the count of associated proteins. apoV, apoptotic vesicle; DEPs, differentially expressed proteins; MSC, mesenchymal stem cell; PLT, platelets.

Modulation of Lipid Metabolism by PLT-ApoVs and MSC-ApoVs

Optimal dosing of apoptotic vesicles was established by testing a range of concentrations (0, 50, 100, 200, and 400 ng/mL). Exposure to PLT-apoVs or MSC-apoVs at levels up to 400 ng/mL in proliferation medium produced no detectable cytotoxicity. As PPARγ represents a central transcriptional regulator of adipocyte differentiation [42, 43], its expression level was monitored in adipogenic medium. Both types of apoVs markedly suppressed

PPARγ transcription, with the 100 ng/mL dose yielding the most robust anti-adipogenic response. This concentration was therefore adopted for all further investigations.

MSCs were subsequently cultured in adipogenic medium supplemented with or without apoVs to examine their influence on differentiation. After 14 days, Oil Red O staining revealed extensive intracellular lipid droplet formation in the adipogenic medium control condition, whereas apoV co-treatment produced a clear reduction in lipid accumulation **(Figures 3a and 3b)**. Quantitative assessment confirmed that PLT-apoV exposure led to significantly fewer lipid droplets than MSC-apoV treatment **(Figures 3a and 3b)**. Consistent with these observations, transcript levels of key adipogenic genes (C/EBPα, LPL, FABP4, and PPARγ) were substantially downregulated upon apoV addition, with PLT-apoVs eliciting stronger repression than MSC-apoVs **(Figure 3c)**.

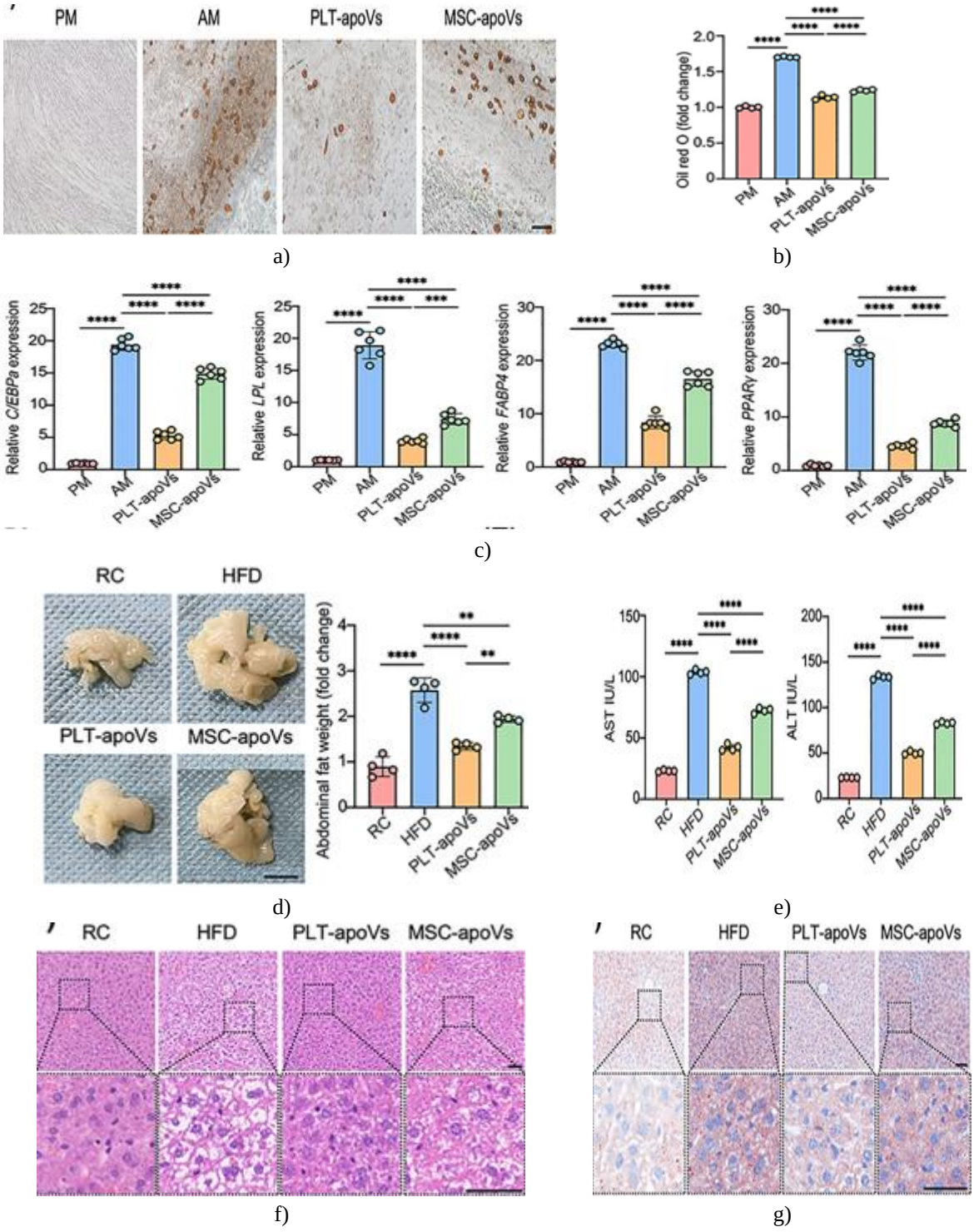

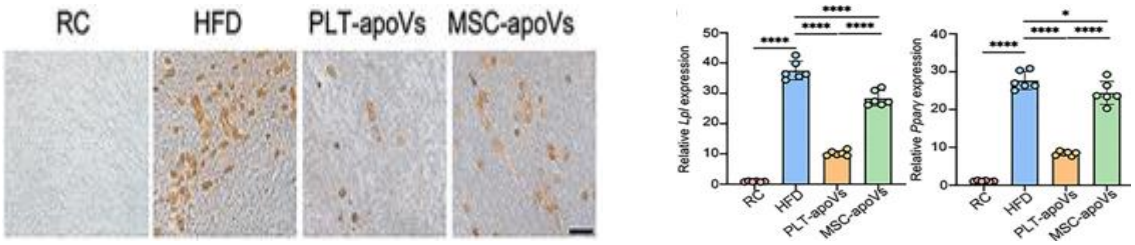

h) i)

Figure 3. Suppressive influence of PLT-apoVs and MSC-apoVs on adipocyte differentiation. MSCs were grown in proliferation medium, adipogenic induction medium (AM), or AM containing 100 ng/mL PLT-apoVs or MSC-apoVs for 14–21 days. Mice were maintained on either a high-fat diet (HFD) or standard chow for 16 weeks. HFD animals were subdivided into three cohorts receiving weekly intravenous administration of PLT-apoVs, MSC-apoVs, or vehicle control. (a, b) Oil Red O staining and corresponding quantification in MSCs following 14 days of culture. Scale bar: 100 μm. (c) mRNA expression of adipogenic markers at 14–21 days. (d) Representative photographs and quantification of abdominal adipose tissue mass. (e) Circulating AST and ALT concentrations. AST, aspartate aminotransferase; ALT, alanine aminotransferase. (f) Hematoxylin and eosin (H&E) staining of hepatic tissue. Scale bar: 100 μm. (g) Oil Red O staining of liver sections. Scale bar: 100 μm. (h) Evaluation of adipogenic differentiation capacity of MSCs isolated from experimental mice by Oil Red O staining. (i) Quantitative RT-qPCR analysis of adipogenic gene expression in mouse-derived MSCs (mMSCs). Results are expressed as mean ± standard deviation. Multiple-group statistical comparisons employed one-way ANOVA followed by Tukey's post hoc test or Welch's ANOVA with Dunnett's T3 post hoc test. AM, adipogenic induction medium; apoV, apoptotic vesicle; HFD, high fat diet; MSC, mesenchymal stem cell; PLT, platelets. *p < .05, **p < .01, ***p < .001, ****p < .0001.

To explore the therapeutic potential of apoVs in non-alcoholic fatty liver disease (NAFLD), HFD-fed mice were randomized into three treatment cohorts and received weekly tail-vein injections of PLT-apoVs, MSC-apoVs, or vehicle. Following eight weeks of intervention, visceral tissue histology displayed no adverse changes, confirming the safety profile of apoV administration. HFD mice exhibited pronounced abdominal fat expansion relative to regular chow controls **(Figures 3d and 3e)**. Successful induction of NAFLD was evidenced by prominent hepatic steatosis on H&E and Oil Red O staining in the HFD group **(Figures 3f and 3g)**. ApoV treatment produced notable reductions in both visceral fat mass and intrahepatic lipid droplets **(Figures 3d–3g)**, with PLT-apoVs achieving greater improvements than MSC-apoVs **(Figures 3f and 3g)**. MSCs isolated from HFD mice displayed enhanced adipogenic potential compared with those from regular chow animals, as indicated by increased lipid droplet formation and elevated adipogenic gene expression. ApoV supplementation effectively counteracted this heightened differentiation capacity, with PLT-apoVs demonstrating superior inhibitory efficacy over MSC-apoVs **(Figures 3h–3i)**.

In summary, both PLT-apoVs and MSC-apoVs effectively modulate lipid metabolism under in vitro and in vivo conditions, yet PLT-apoVs confer more pronounced protective effects against the development of NAFLD.

Suppression of mesenchymal stem cell adipogenesis by ApoVs through APOA2 upregulation

From the top ten proteins showing increased abundance in PLT-apoVs versus MSC-apoVs, APOA2 drew particular interest for several reasons: it displayed the largest fold enrichment **(Figure 4a)**, its expression pattern matched the quantitative proteomic results **(Figures 4b and 4c)**, and it functions as a core lipoprotein constituent primarily responsible for high-density lipoprotein (HDL) formation and low-density lipoprotein breakdown in humans [44-46]. Immunogold electron microscopy further verified higher APOA2 incorporation in PLT-apoVs than in MSC-apoVs **(Figure 4d)**. Treatment with apoVs elevated APOA2 protein levels in MSCs, counteracting adipogenic progression, with PLT-apoVs inducing a stronger response than MSC-apoVs **(Figure 4e)**. On the basis of these observations, APOA2 was considered likely to mediate the regulatory influence of apoVs on MSC adipogenic differentiation.

Protein	PLT-apoVs VS MSC-apoVs	log_2(fold change)	Q value
APOA2	**Up**	**3.320258555**	**4.75E-24**
NECAB2	Up	3.308597937	1.06E-16
CLDN5	Up	3.276980178	1.12E-13
ZNF132	Up	3.273047541	1.51E-12
CACNA1C	Up	3.226213852	4.19E-11
FCER1G	Up	3.222531313	5.54E-12
IGLV1-51	Up	3.200222835	4.32E-13
ACKR2	Up	3.175347528	1.15E-07
TRANK1	Up	3.172720668	1.03E-11
CREB5	Up	3.171715734	1.12E-11

a)

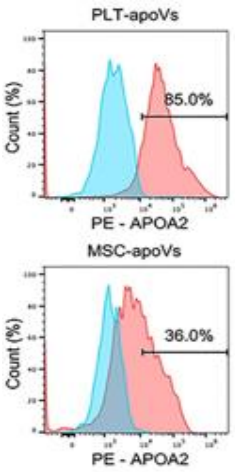

b)

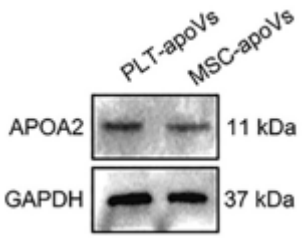

c)

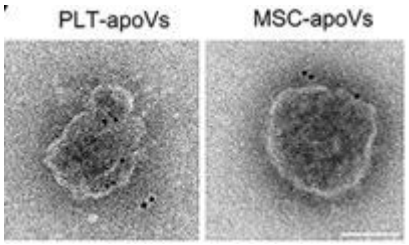

d)

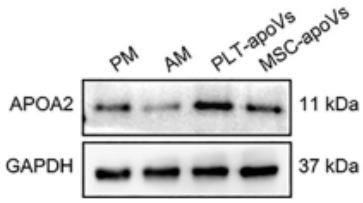

e)

Figure 4. Identification of APOA2 as a candidate factor involved in apoV-mediated control of adipogenesis. MSCs were maintained under proliferation medium conditions, adipogenic induction medium (AM), or AM supplemented with 100 ng/mL PLT-apoVs or MSC-apoVs for 14–21 days. (a) Top ten upregulated proteins in PLT-apoVs relative to MSC-apoVs according to quantitative proteomics. (b) Flow cytometry measurement of APOA2 expression in PLT-apoVs and MSC-apoVs. (c) Western blot determination of APOA2 abundance in PLT-apoVs and MSC-apoVs. (d) Immunogold labeling visualization of APOA2 enrichment in PLT-apoVs and MSC-apoVs. Scale bar: 100 nm. (e) Western blot analysis of APOA2 protein levels in treated MSCs. AM, adipogenic induction medium; apoV, apoptotic vesicle; MSC, mesenchymal stem cell; PLT, platelets.

To test this possibility, magnetic-activated cell sorting was utilized to isolate the APOA2-negative fraction of PLT-apoVs ($APOA2^-$ apoVs) [22]. Sorting purity was confirmed through flow cytometric evaluation. Functional studies showed that depletion of APOA2 markedly diminished the ability of PLT-apoVs to restrain adipogenic differentiation in cultured MSCs **(Figures 5a–5d)** and to attenuate NAFLD progression in animal models **(Figures 5e–5h)**. These findings underscore the central contribution of APOA2 to apoV-dependent lipid metabolic control. PLT-apoV exposure increased APOA2 protein content within MSCs, whereas this elevation was attenuated when APOA2-depleted vesicles were used **(Figure 5d)**. Notably, APOA2 transcript levels remained unaltered **(Figure 5c)**, suggesting that MSCs acquire the protein directly from internalized apoVs rather than through transcriptional activation.

Additional experiments involved generating APOA2-overexpressing MSCs via lentiviral transduction and isolating the corresponding apoVs ($APOA2^+$ apoVs). Successful enrichment was confirmed by western blotting. When MSCs were exposed to these APOA2-enriched vesicles, their anti-adipogenic potency was significantly enhanced compared with standard MSC-apoVs, demonstrating that APOA2 abundance augments the vesicles' capacity to limit adipocyte formation. In vivo, APOA2-overexpressing apoVs provided improved protection against NAFLD development. Again, APOA2 protein levels in recipient MSCs reflected the content supplied by the apoVs, while gene expression showed no meaningful variation. This pattern reinforces the notion that target cells incorporate functional APOA2 protein delivered by the apoptotic vesicles.

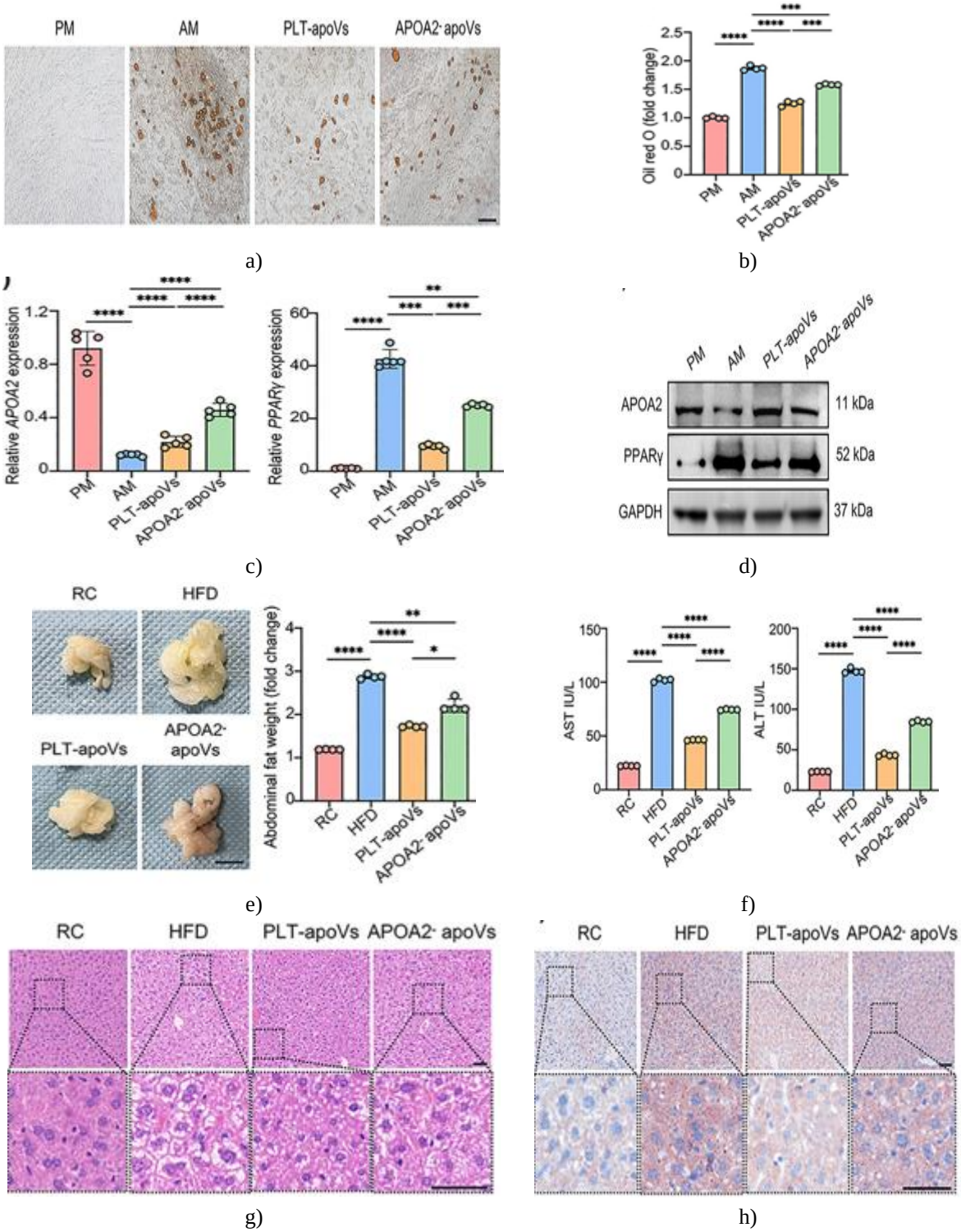

Figure 5. Critical involvement of APOA2 in the anti-adipogenic mechanism of PLT-apoVs. MSCs were cultured in proliferation medium, adipogenic induction medium (AM), or AM containing 100 ng/mL PLT-apoVs or the APOA2-negative subpopulation (APOA2⁻ apoV group) for 14–21 days. Mice underwent 16 weeks of paired feeding with either a high-fat diet (HFD) or regular chow (RC). HFD mice were randomly divided into three treatment arms and given weekly tail vein injections of PLT-apoVs, APOA2⁻ apoVs, or vehicle. (a, b) Evaluation of intracellular lipid accumulation in MSCs by Oil Red O staining and quantitative measurement. Scale bar: 100 μm. (c) RT-qPCR quantification of adipogenic gene transcripts. (d) Western blot analysis of key regulatory proteins. (e) Gross appearance and quantification of abdominal fat. (f) Serum concentrations of AST and ALT in experimental mice. AST: aspartate aminotransferase; ALT: alanine aminotransferase. Liver sections were examined for lipid deposition using H&E staining (g) and Oil Red O

staining (h). Scale bar: 100 μm. Data represent mean ± standard deviation. Inter-group differences were assessed by one-way ANOVA with Tukey's post hoc test or Welch's ANOVA with Dunnett's T3 post hoc test. AM, adipogenic induction medium; apoV, apoptotic vesicle; HFD, high fat diet; MSC, mesenchymal stem cell; PLT, platelets. *p < .05, **p < .01, ***p < .001, ****p < .0001.

Taken together, these experiments establish APOA2 as a major mediator through which apoVs inhibit adipogenic differentiation of mesenchymal stem cells and exert beneficial effects against NAFLD.

APOA2-engineered ApoVs exhibit enhanced capacity to inhibit adipogenesis

To further evaluate the practical utility of APOA2, the protein was successfully incorporated into apoVs via sonication. Western blotting confirmed effective protein loading into the vesicles. Functional evaluation revealed that PLT-apoVs carrying additional APOA2 (APOA2-PLT-apoVs group) displayed markedly greater suppression of MSC adipogenic differentiation in culture than their unmodified counterparts. Parallel results were observed when comparing APOA2-loaded MSC-apoVs with native MSC-apoVs **(Figures 6a–6c)**. In the animal model, APOA2-enriched apoVs likewise demonstrated improved control over visceral lipid accumulation and yielded better therapeutic benefits against NAFLD than standard apoV preparations **(Figures 6d and 6e)**.

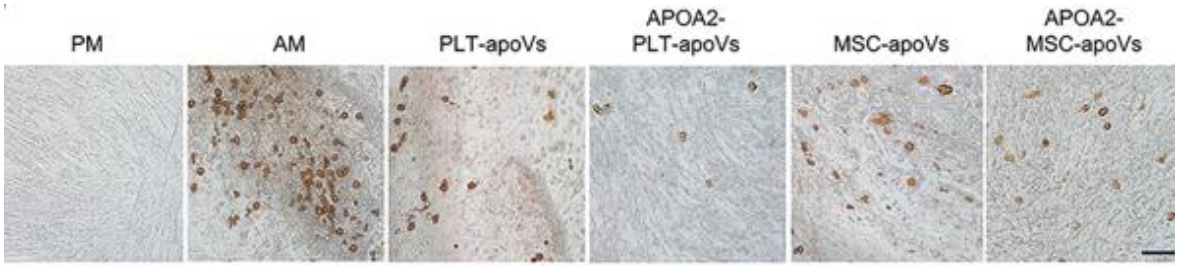

a)

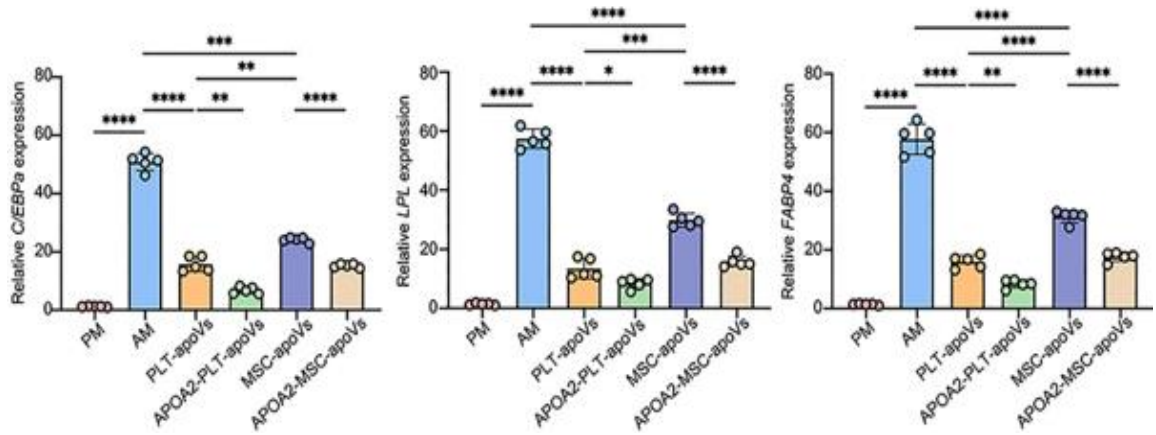

b)

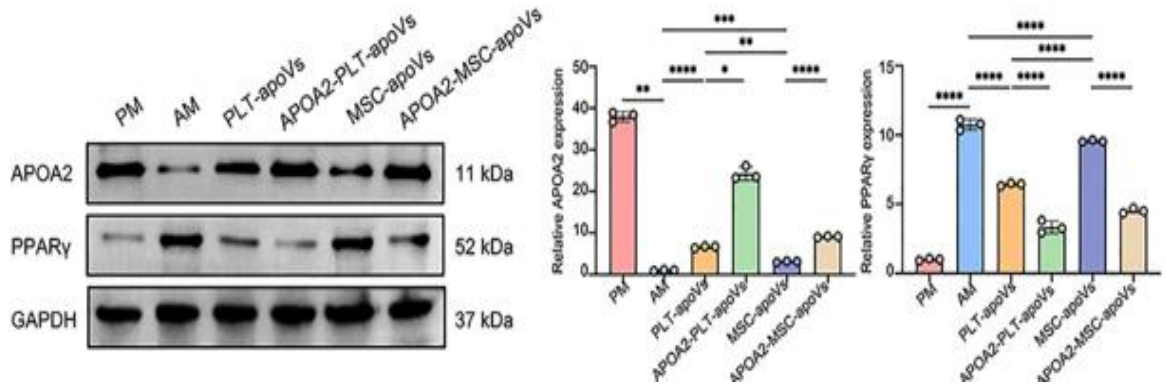

c)

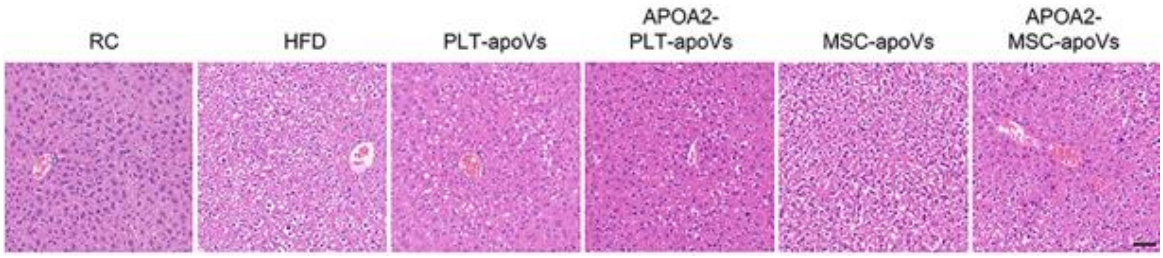

d)

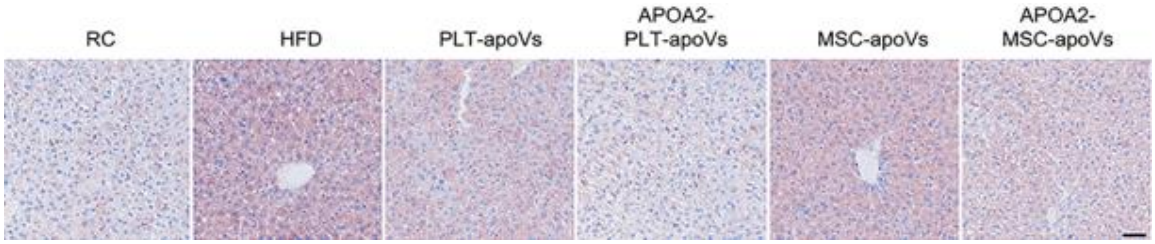

e)

Figure 6. Engineered apoVs show stronger anti-adipogenic activity than native apoV populations. MSCs were maintained in proliferation medium, adipogenic induction medium (AM), or AM containing 200 ng/mL of PLT-apoVs, APOA2-PLT-apoVs, MSC-apoVs, or APOA2-MSC-apoVs for 14–21 days. Mice underwent 16 weeks of paired feeding on either high-fat diet (HFD) or regular chow (RC). HFD-fed mice were randomly allocated to five experimental arms and administered weekly tail-vein injections of PLT-apoVs, engineered PLT-apoVs, MSC-apoVs, engineered MSC-apoVs, or vehicle control. (a) Visualization of lipid droplets within MSCs. Scale bar: 100 μm. (b) Quantitative analysis of adipogenic gene transcripts. (c) Levels of critical regulatory proteins. (d) Histological examination of liver tissue by H&E staining. (e) Assessment of lipid accumulation in the liver. Scale bar: 100 μm. Data are presented as mean ± standard deviation. Statistical evaluation for multiple groups was performed using one-way ANOVA with Tukey's post hoc test or Welch's ANOVA with Dunnett's T3 post hoc test. AM, adipogenic induction medium; apoV, apoptotic vesicle; HFD, high fat diet; MSC, mesenchymal stem cell; PLT, platelets. *p < .05, **p < .01, ***p < .001, ****p < .0001.

Taken together, these findings establish APOA2 as an important modulator within apoVs that influences adipogenesis and highlight its value as a molecular target for boosting the effectiveness of apoptotic vesicle-based therapies in lipid-related metabolic disorders.

The relationship between platelets and non-alcoholic fatty liver disease (NAFLD) is highly complex. First, platelets participate actively in inflammatory processes; NAFLD patients often exhibit elevated mean platelet volume, suggesting heightened platelet activation during inflammation [47]. Second, platelets contribute significantly to coagulation; individuals with NAFLD face increased risk of coagulation abnormalities, and platelet activation can promote thrombus formation, thereby worsening hepatic microcirculatory dysfunction and hepatocyte injury [48]. Third, certain antiplatelet agents have shown promise in NAFLD management; for instance, aspirin can mitigate virus-specific cytotoxic T lymphocyte-mediated hepatic inflammation and fibrosis by suppressing platelet activation pathways [49]. The present study extends these insights by demonstrating that PLT-derived apoptotic vesicles possess substantial therapeutic value in NAFLD treatment, thereby deepening understanding of the multifaceted interplay between platelets and this metabolic liver disorder.

The molecular cargo of apoptotic vesicles reflects the biological characteristics of their parent cells and is closely linked to their functional properties [50]. Building upon observed functional distinctions between PLT-apoVs and MSC-apoVs, we conducted proteomic profiling to comprehensively characterize their protein composition. This approach led to the identification of APOA2 as a promising regulator of apoV-mediated control of MSC adipogenesis. High-density lipoprotein (HDL) is well recognized for its central role in reverse cholesterol transport, which involves the mobilization of cholesterol from peripheral tissues to the liver for excretion [51, 52]. APOA2 constitutes the second most abundant protein in HDL particles; however, its precise contributions to HDL function and lipoprotein metabolism remain incompletely elucidated [53]. Recent studies have highlighted that APOA2 deficiency causes significant remodeling of lipoprotein particles and redistribution of apolipoproteins,

underscoring its importance in lipoprotein metabolism [44-46]. Nevertheless, the role of APOA2 in mesenchymal stem cells has received limited attention. To our knowledge, no prior reports have described the function of APOA2 within apoptotic vesicles. Our mechanistic investigations revealed a direct correlation between APOA2 content in apoVs and their capacity to regulate MSC adipogenesis. Through complementary in vitro and in vivo experiments, we established APOA2 as a critical mediator of apoV-dependent lipid metabolic regulation.

Given that targeted engineering of extracellular vesicles can markedly improve delivery efficiency, cellular targeting, and overall therapeutic efficacy [54], we sought to develop optimized apoVs with enhanced and consistent biological activity. Among passive loading techniques—including incubation, electroporation, and mechanical approaches such as freeze-thaw cycles, sonication, and extrusion—sonication demonstrated superior protein incorporation efficiency [40, 55]. Successful loading of APOA2 was confirmed experimentally. Collectively, our results indicate that APOA2-enriched apoVs more effectively mitigate NAFLD by suppressing lipid accumulation in mesenchymal stem cells. This engineering strategy offers a promising direction for advancing apoV-based interventions in lipid metabolism disorders.

Conclusion

In summary, this study confirms the therapeutic efficacy of PLT-apoVs against NAFLD, identifies APOA2 as a key functional regulator in apoV-mediated lipid metabolism, and successfully employs it as a target for apoV modification. More broadly, APOA2-enriched apoV populations exhibit superior therapeutic performance in alleviating NAFLD, thereby establishing a framework for enhancing apoV efficacy through strategic enrichment of specific regulatory molecules.

Despite the advantages of high-fat diet (HFD) feeding in mice, which closely recapitulates key histopathological and pathogenic features of human NAFLD compared with alternative models [56], certain limitations should be acknowledged. HFD feeding primarily induces hepatic steatosis, while progression to non-alcoholic steatohepatitis (NASH) and hepatocellular carcinoma (HCC) generally requires additional insults in current animal models [57]. Furthermore, HFD formulations vary considerably in composition and duration, leading to differential responses across genetically diverse mouse strains [58]. Alternative dietary models that promote NASH, such as fast-food-style or high-fat high-fructose diets, encounter similar challenges, including a lack of standardized protocols [59]. Future research would benefit from animal models that integrate multiple pathogenic factors to more accurately replicate human NAFLD and facilitate discovery of novel therapeutic approaches.

Acknowledgments: None

Conflict of Interest: None

Financial Support: None

Ethics Statement: None

References

1. Pan K, Xu J, Xu Y, Wang C, Yu J. The association between endocrine disrupting chemicals and nonalcoholic fatty liver disease: A systematic review and meta-analysis. Pharmacol Res. 2024;205:107251.
2. Tangestani H, Jamshidi A, Farhadi A, Ghalandari H, Dehghani P, Moghaddas N, et al. The effects of pomegranate (Punica granatum) on nonalcoholic fatty liver disease: A systematic review of in vivo interventional studies. Phytother Res. 2024;38(8):4189-205.
3. Liu X, Pan Q, Cao H, Xin F, Zhao Z, Yang R, et al. Lipotoxic hepatocyte-derived exosomal microRNA 192-5p activates macrophages through Rictor/Akt/Forkhead box transcription factor O1 signaling in nonalcoholic fatty liver disease. Hepatology. 2020;72:454-68.
4. Yang F, Wu Y, Chen Y, Xi J, Chu Y, Jin J, et al. Human umbilical cord mesenchymal stem cell-derived exosomes ameliorate liver steatosis by promoting fatty acid oxidation and reducing fatty acid synthesis. JHEP Rep. 2023;5(7):100746.
5. Hou X, Yin S, Ren R, Liu S, Yong L, Liu Y, et al. Myeloid-cell-specific IL-6 signaling promotes microRNA-223-enriched exosome production to attenuate NAFLD-associated fibrosis. Hepatology. 2021;74(1):116-30.

6. Nevola R, Epifani R, Imbriani S, Tortorella G, Aprea C, Galiero R, et al. GLP-1 receptor agonists in non-alcoholic fatty liver disease: current evidence and future perspectives. Int J Mol Sci. 2023;24(2):1703.
7. Pan Q, Lin S, Li Y, Liu L, Li X, Gao X, et al. A novel GLP-1 and FGF21 dual agonist has therapeutic potential for diabetes and non-alcoholic steatohepatitis. EBioMedicine. 2021;63:103202.
8. Tacke F, Puengel T, Loomba R, Friedman SL. An integrated view of anti-inflammatory and antifibrotic targets for the treatment of NASH. J Hepatol. 2023;79(2):552-66.
9. Zhang C, Yang M. Current options and future directions for NAFLD and NASH treatment. Int J Mol Sci. 2021;22(14):7571.
10. Safari Z, Gérard P. The links between the gut microbiome and non-alcoholic fatty liver disease (NAFLD) Z. Safari, P. Gérard. Cell Mol Life Sci. 2019;76(8):1541-58.
11. Zhang X, Coker OO, Chu ES, Fu K, Lau HCH, Wang Y, et al. Dietary cholesterol drives fatty liver-associated liver cancer by modulating gut microbiota and metabolites. Gut. 2021;70(4):761-74.
12. Tarantino G, Balsano C, Santini SJ, Brienza G, Clemente I, Cosimini B, et al. It is high time physicians thought of natural products for alleviating NAFLD. Is there sufficient evidence to use them. Int J Mol Sci. 2021;22(24):13424.
13. Guo X, Yin X, Liu Z, Wang J. Non-alcoholic fatty liver disease (NAFLD) pathogenesis and natural products for prevention and treatment. Int J Mol Sci. 2022;23(24):15489.
14. Wang L, Yan Y, Wu L, Peng J. Natural products in non-alcoholic fatty liver disease (NAFLD): Novel lead discovery for drug development. Pharmacol Res. 2023;196:106925.
15. Szabo G. Exosomes and MicroRNA-223 at the Intersection of Inflammation and Fibrosis in NAFLD. Hepatology. 2021;74(1):5-8.
16. Hu L, Yin C, Zhao F, Ali A, Ma J, Qian A. Mesenchymal stem cells: cell fate decision to osteoblast or adipocyte and application in osteoporosis treatment. Int J Mol Sci. 2018;19(2):360.
17. Kholodenko IV, Yarygin KN. Hepatic macrophages as targets for the MSC-based cell therapy in non-alcoholic steatohepatitis. Biomedicines. 2023;11(11):3056.
18. Neshat SY, Quiroz VM, Wang Y, Tamayo S, Doloff JC. Liver disease: induction, progression, immunological mechanisms, and therapeutic interventions. Int J Mol Sci. 2021;22(13):6777.
19. Zhu Y, Yang K, Cheng Y, Liu Y, Gu R, Liu X, et al. Apoptotic vesicles regulate bone metabolism via the miR1324/SNX14/SMAD1/5 signaling axis. Small. 2023;19(16):e2205813.
20. Liu H, Liu S, Qiu X, Yang X, Bao L, Pu F, et al. Donor MSCs release apoptotic bodies to improve myocardial infarction via autophagy regulation in recipient cells. Autophagy. 2020;16(12):2140-61.
21. Liu S, Jiang L, Li H, Shi H, Luo H, Zhang Y, et al. Mesenchymal stem cells prevent hypertrophic scar formation via inflammatory regulation when undergoing apoptosis. J Invest Dermatol. 2014;134(10):2648-58.
22. Zhang X, Tang J, Kou X, Huang W, Zhu Y, Jiang Y, et al. Proteomic analysis of MSC-derived apoptotic vesicles identifies Fas inheritance to ameliorate haemophilia A via activating platelet functions. J Extracell Vesicles. 2022;11(7):e12240.
23. Cao Z, Li P, Li Y, Zhang M, Hao M, Li W, et al. Encapsulation of nano-bortezomib in apoptotic stem cell-derived vesicles for the treatment of multiple myeloma. Small. 2023;19(40):2301748.
24. Shao Y, Jiang Y, Yang K, Zhu Y, Liu Y, Zhang P, et al. Apoptotic vesicles derived from human red blood cells promote bone regeneration via carbonic anhydrase 1. Cell Prolif. 2024;57(2):e13547.
25. Saumell-Esnaola M, Delgado D, García Del Caño G, Beitia M, Sallés J, González-Burguera I, et al. Isolation of platelet-derived exosomes from human platelet-rich plasma: biochemical and morphological characterization. Int J Mol Sci. 2022;23(5):2861.
26. Fu Y, Zhang M, Sui B, Yuan F, Zhang W, Weng Y, et al. Mesenchymal stem cell-derived apoptotic vesicles ameliorate impaired ovarian folliculogenesis in polycystic ovary syndrome and ovarian aging by targeting WNT signaling. Theranostics. 2024;14(8):3385-410.
27. Sui B, Wang R, Chen C, Kou X, Wu D, Fu Y, et al. Apoptotic vesicular metabolism contributes to organelle assembly and safeguards liver homeostasis and regeneration. Gastroenterology. 2024;167:343-60.
28. Xiang L, An Z, Wu X, Wang J, Cai S, Lu Y, et al. Carbon dot-loaded apoptotic vesicles improve the liver Kupffer cell-mediated antibacterial effect to synergistically alleviate sepsis. ACS Nano. 2024;18(26):16726-47.

29. Ma L, Chen C, Liu D, Huang Z, Li J, Liu H, et al. Apoptotic extracellular vesicles are metabolized regulators nurturing the skin and hair. Bioact Mater. 2022;19:626-42.
30. Cheng Y, Zhu Y, Liu Y, Liu X, Ding Y, Li D, et al. Tailored apoptotic vesicles promote bone regeneration by releasing the osteoinductive brake. Int J Oral Sci. 2024;16(1):31.
31. Zheng C, Sui B, Zhang X, Hu J, Chen J, Liu J, et al. Apoptotic vesicles restore liver macrophage homeostasis to counteract type 2 diabetes. J Extracell Vesicles. 2021;10(7):e12109.
32. Jiang Y, Zhu Y, Shao Y, Yang K, Zhu L, Liu Y, et al. Platelet-derived apoptotic vesicles promote bone regeneration via Golgi phosphoprotein 2 (GOLPH2)-AKT signaling axis. ACS Nano. 2023;17(24):25070-88.
33. Chen S, Tang Y, Liu Y, Zhang P, Lv L, Zhang X, et al. Exosomes derived from miR-375-overexpressing human adipose mesenchymal stem cells promote bone regeneration. Cell Prolif. 2019;52(5):e12669.
34. Noble JM, Roberts LM, Vidavsky N, Chiou AE, Fischbach C, Paszek MJ, et al. Direct comparison of optical and electron microscopy methods for structural characterization of extracellular vesicles. J Struct Biol. 2020;210(1):107474.
35. Haraszti RA, Didiot MC, Sapp E, Leszyk J, Shaffer SA, Rockwell HE, et al. High-resolution proteomic and lipidomic analysis of exosomes and microvesicles from different cell sources. J Extracell Vesicles. 2016;5:32570.
36. Ma X, Fan C, Wang Y, Du Y, Zhu Y, Liu H, et al. MiR-137 knockdown promotes the osteogenic differentiation of human adipose-derived stem cells via the LSD1/BMP2/SMAD4 signaling network. J Cell Physiol. 2020;235(1):909-24.
37. Li W, Liu Y, Zhang P, Tang Y, Zhou M, Jiang W, et al. Tissue-engineered bone immobilized with human adipose stem cells-derived exosomes promotes bone regeneration. ACS Appl Mater Interfaces. 2018;10(6):5240-52.
38. Du Y, Zhang M, Liu X, Li Z, Hu M, Tian Y, et al. CDC20 promotes bone formation via APC/C dependent ubiquitination and degradation of p65. EMBO Rep. 2021;22(9):e52576.
39. Zhu Y, Zhang X, Gu R, Liu X, Wang S, Xia D, et al. LAMA2 regulates the fate commitment of mesenchymal stem cells via hedgehog signaling. Stem Cell Res Ther. 2020;11(1):135.
40. Haney MJ, Klyachko NL, Zhao Y, Gupta R, Plotnikova EG, He Z, et al. Exosomes as drug delivery vehicles for Parkinson's disease therapy. J Control Release. 2015;207:18-30.
41. Kim KE, Lee J, Shin HJ, Jeong EA, Jang HM, Ahn YJ, et al. Lipocalin-2 activates hepatic stellate cells and promotes nonalcoholic steatohepatitis in high-fat diet-fed Ob/Ob mice. Hepatology. 2023;77(3):888-904.
42. Prasad P, Cancelas JA. From marrow to bone and fat: Exploring the multifaceted roles of leptin receptor positive bone marrow mesenchymal stromal cells. Cells. 2024;13(11):910.
43. Kim HY, Kim HS. Podoplanin depletion in tonsil-derived mesenchymal stem cells induces cellular senescence via regulation of the p16Ink4a/Rb pathway. Cell Commun Signal. 2024;22(1):323.
44. Lai CQ, Smith CE, Parnell LD, Lee YC, Corella D, Hopkins P, et al. Epigenomics and metabolomics reveal the mechanism of the APOA2-saturated fat intake interaction affecting obesity. Am J Clin Nutr. 2018;108:188-200.
45. Dai J, Li Y, Kametani F, Cui X, Igarashi Y, Huo J, et al. Curcumin promotes AApoAII amyloidosis and peroxisome proliferation in mice by activating the PPARα signaling pathway. Elife. 2021;10:e63538.
46. Yang M, Liu Y, Dai J, Li L, Ding X, Xu Z, et al. Apolipoprotein A-II induces acute-phase response associated AA amyloidosis in mice through conformational changes of plasma lipoprotein structure. Sci Rep. 2018;8(1):5620.
47. Patel K, Asrani SK, Fiel MI, Levine D, Leung DH, Duarte-Rojo A, et al. Accuracy of blood-based biomarkers for staging liver fibrosis in chronic liver disease: A systematic review supporting the AASLD Practice Guideline. Hepatology. 2025;81(1):358-83.
48. Mathew JF, Panackel C, Jacob M, Ramesh G, John N. A validation study of non-invasive scoring systems for assessing severity of hepatic fibrosis in a cohort of South Indian patients with non-alcoholic fatty liver disease. J Clin Exp Hepatol. 2024;14(5):101407.
49. Boccatonda A, Del Cane L, Marola L, D'Ardes D, Lessiani G, di Gregorio N, et al. Platelet, antiplatelet therapy and metabolic dysfunction-associated steatotic liver disease: a narrative review. Life. 2024;14(4):473.
50. Jiang T, Xia Y, Wang W, Zhao J, Liu W, Liu S, et al. Apoptotic bodies inhibit inflammation by PDL1–PD1-mediated macrophage metabolic reprogramming. Cell Prolif. 2024;57(1):e13531.

51. Osei-Hwedieh DO, Amar M, Sviridov D, Remaley AT. Apolipoprotein mimetic peptides: Mechanisms of action as anti-atherogenic agents. Pharmacol Ther. 2011;130(1):83-94.
52. Escola-Gil JC, Calpe-Berdiel L, Palomer X, Ribas V, Ordonez-Llanos J, Blanco-Vaca F. Antiatherogenic role of high-density lipoproteins: insights from genetically engineered-mice. Front Biosci. 2006;11:1328-34.
53. Blanco-Vaca F, Escolà-Gil JC, Martín-Campos JM, Julve J. Role of apoA-II in lipid metabolism and atherosclerosis: advances in the study of an enigmatic protein. J Lipid Res. 2001;42(11):1727-39.
54. Ma T, Wang M, Wang S, Hu H, Zhang X, Wang H, et al. BMSC derived EVs inhibit colorectal Cancer progression by transporting MAGI2-AS3 or something similar. Cell Signal. 2024;121:111235.
55. Kim MS, Haney MJ, Zhao Y, Mahajan V, Deygen I, Klyachko NL, et al. Development of exosome-encapsulated paclitaxel to overcome MDR in cancer cells. Nanomedicine. 2016;12(3):655-64.
56. Soret PA, Magusto J, Housset C, Gautheron J. In vitro and in vivo models of non-alcoholic fatty liver disease: a critical appraisal. J Clin Med. 2020;10(1):36.
57. Basha A, May SC, Anderson RM, Samala N, Mirmira RG. Non-alcoholic fatty liver disease: translating disease mechanisms into therapeutics using animal models. Int J Mol Sci. 2023;24(12):9996.
58. Chua D, Low ZS, Cheam GX, Ng AS, Tan NS. Utility of human relevant preclinical animal models in navigating NAFLD to MAFLD paradigm. Int J Mol Sci. 2022;23(23):14762.
59. Flessa C, Nasiri-Ansari N, Kyrou I, Leca B, Lianou M, Chatzigeorgiou A, et al. Genetic and diet-induced animal models for non-alcoholic fatty liver disease (NAFLD) research. Int J Mol Sci. 2022;23(24):15791.